

## Magnetic Structure of $^{17}\text{O}$ at High Momentum

N. Kalantar-Nayestanaki,<sup>(a)</sup> H. Baghaei,<sup>(b)</sup> W. Bertozzi, S. Dixit,<sup>(c)</sup> J. M. Finn,<sup>(d)</sup> C. E. Hyde-Wright,<sup>(e)</sup>  
S. Kowalski, R. W. Lourie, C. P. Sargent, P. E. Ulmer,<sup>(d)</sup> and L. Weinstein

*Department of Physics and Laboratory for Nuclear Science, Massachusetts Institute of Technology,  
Cambridge, Massachusetts 02139*

M. V. Hynes

*Los Alamos National Laboratory, Los Alamos, New Mexico 87545*

B. L. Berman

*Department of Physics, George Washington University, Washington, D.C. 20052*

and

J. J. Kelly

*Department of Physics and Astronomy, University of Maryland, College Park, Maryland 20742*

(Received 12 November 1986; revised manuscript received 20 October 1987)

The elastic magnetic form factor of  $^{17}\text{O}$  has been measured for effective momentum transfers  $2.47 \leq q_{\text{eff}} \leq 3.65 \text{ fm}^{-1}$  by electron scattering. The form factor drops by almost three decades in this range. The data follow an extreme single-particle Woods-Saxon shell-model calculation. Many-body effects such as meson-exchange currents or core polarization do not seem to play a significant role in the  $q$  range of this experiment.

PACS numbers: 25.30.Bf, 27.20.+n

The shell model has been very successful in explaining the structure of many nuclei. In particular, the magnetic properties of nuclei with one nucleon outside a closed shell should be explained by the properties of that single-particle orbital outside the closed shell. A good case to study is  $^{17}\text{O}$ , which has one neutron in the  $d_{5/2}$  orbital outside the doubly closed  $^{16}\text{O}$  nucleus. The static magnetic moment of this nucleus is  $-1.894\mu_N$ ,<sup>1</sup> which is very close to the Schmidt value of  $-1.913\mu_N$ , and the spectroscopic strength for the  $d_{5/2}$  orbital as determined by  $^{16}\text{O}(d,p)^{17}\text{O}$  reactions<sup>2</sup> and heavy-ion elastic scattering<sup>3</sup> is about 90% of the full single-particle strength. However, both the large static quadrupole moment of  $^{17}\text{O}$  ( $-2.578 e \text{ fm}^2$ )<sup>1</sup> and the large  $E2$  transition matrix element to the first excited state ( $0.871 \text{ MeV}$ ,  $J^\pi = \frac{1}{2}^+$ )<sup>4</sup> indicate that the  $^{16}\text{O}$  core, as well as the valence neutron, plays a role in the dynamics of  $^{17}\text{O}$ . Calculations of core polarization (CP) and meson-exchange currents (MEC) show that these two effects cancel in the static magnetic moment.<sup>5</sup> However, CP does create a static quadrupole moment for  $^{17}\text{O}$ . These processes are then expected to influence the behavior of the magnetization of  $^{17}\text{O}$  at nonzero momentum transfers. A particularly advantageous region to examine the magnetic structure for effects such as CP and two-body MEC is  $2.8 \leq |\mathbf{q}| \leq 4.0 \text{ fm}^{-1}$ , where the elastic single-particle amplitudes for all multipoles are expected to have a common minimum (see Fig. 1).

The experiment was performed at the Massachusetts

Institute of Technology Bates Linear Accelerator Center with the high-resolution energy-loss spectrometer system (ELSSY).<sup>8</sup> This experiment was an extension of a previous experiment done at the same laboratory, but at lower momentum transfers, by Hynes *et al.*<sup>6</sup> Forward-angle measurements were made with use of the targets of Ref. 6. Backwards-angle measurements were made with new Be  $^{17}\text{O}$  targets with thicknesses ranging between 50 and  $110 \text{ mg/cm}^2$  manufactured at Lawrence Livermore National Laboratory. All the targets were used in transmission geometry, with the normal to the target bisecting the scattering angle. The abundances of different oxygen isotopes in the new targets as determined by mass spectroscopy before the fabrication of the target were 51.3%, 31.6%, and 17.1% for  $^{17}\text{O}$ ,  $^{18}\text{O}$ , and  $^{16}\text{O}$ , respectively. These values were determined independently during the experiment by the method given by Norum *et al.*,<sup>9</sup> and the experimental  $^{17}\text{O}$  abundance agreed with the mass-spectroscopy results. For the analysis of the data, the mass-spectroscopic values were used since they are more precise. An average electron-beam current of  $10\text{--}20 \mu\text{A}$  was used. The energies and the angles used in this experiment are shown in Table I. In addition, forward-angle measurements of elastic scattering were made on Be  $^{16}\text{O}$  and  $^{12}\text{C}$  to provide the absolute normalization of the data. Another point for comparison is the  $^{17}\text{O}$  datum at  $|\mathbf{q}| = 2.47 \text{ fm}^{-1}$  which is consistent with the result of Ref. 6.

The electron-scattering cross section can be approxi-

mated with the first Born approximation (and plane waves)<sup>10</sup>:

$$d\sigma/d\Omega = Z^2 \sigma_{\text{Mott}} \eta \{ (q_\mu^4/|\mathbf{q}|^4) |F_L|^2 + [ -\frac{1}{2} q_\mu^2/|\mathbf{q}|^2 + \tan^2(\frac{1}{2}\theta) ] |F_T|^2 \}, \quad (1)$$

where  $d\sigma/d\Omega$  is the laboratory cross section,  $Z$  is the atomic number of the target nucleus,  $\sigma_{\text{Mott}} = \alpha^2 \cos^2(\frac{1}{2}\theta)/4E_0^2 \sin^4(\frac{1}{2}\theta)$  is the Mott cross section,  $\alpha$  is the fine-structure constant,  $\theta$  is the laboratory scattering angle,  $E_0$  is the incident electron energy,  $\eta = [1 + (2E_0/M)\sin^2(\frac{1}{2}\theta)]^{-1}$  is the recoil factor, and  $M$  is the mass of the target nucleus.  $F_L$  is the longitudinal form factor and  $F_T$  is the transverse form factor, and  $|F_T|^2 = |F_M|^2 + |F_E|^2$ . For elastic scattering, the electric form factor  $F_E = 0$ ; thus only  $F_L$  and the magnetic form factor  $F_M$  contribute to the cross section.<sup>10</sup> The momentum transfer  $|\mathbf{q}|$  ( $\equiv q$ ) is given by  $|\mathbf{q}|^2 = \omega^2 - q_\mu^2$ , where  $\omega$  is the energy and  $q_\mu$  is the four-momentum transferred to the nucleus:  $q_\mu^2 = -4E_0 E_f$

$\times \sin^2(\frac{1}{2}\theta)$ , where  $E_f$  is the final energy,  $E_f = E_0 - \omega$ . For elastic scattering,  $q_\mu^2 = -4E_0^2 \eta \sin^2(\frac{1}{2}\theta)$ . To first order, the Coulomb distortion of the electrons increases the momentum transfer, yielding an effective momentum transfer  $q_{\text{eff}}$  given by<sup>11</sup>

$$q_{\text{eff}} = q [1 + \frac{3}{2} (\frac{3}{5})^{1/2} Z\alpha/E_0 \langle r^2 \rangle^{1/2}],$$

where  $\langle r^2 \rangle^{1/2}$  is the rms charge radius of the target nucleus. For the  $q$  range of the present experiment, when a distorted-wave calculation for the magnetic form factor at  $q_{\text{eff}}$  is compared with a plane-wave calculation at  $q$ , the largest difference in the total form factor is about 5%. Therefore, for convenience, the data at  $q_{\text{eff}}$  are compared with the plane-wave form factor at  $q$ .

The results of this experiment along with the previous data for  $0.55 \leq |\mathbf{q}| \leq 2.74 \text{ fm}^{-1}$  from Ref. 6 are presented in Fig. 1 and the present results are also tabulated in Table I. Note that there is a point at  $2.47 \text{ fm}^{-1}$  from this experiment which overlaps with the results of Ref. 6. The squared transverse form factor  $|F_M|^2$  is obtained from relation (1) by performance of a Rosenbluth separation, in which  $|F_L|^2 + [\frac{1}{2} + \tan^2(\frac{1}{2}\theta)] |F_M|^2$  is plotted against  $\frac{1}{2} + \tan^2(\frac{1}{2}\theta)$  and the slope of the line is  $|F_M|^2$ . (Note that for the kinematics of this experiment,  $q_\mu^2 \approx -|\mathbf{q}|^2$ .) The spin-parity assignment of  $^{17}\text{O}$  is  $J^\pi = \frac{5}{2}^+$ . Therefore, for elastic scattering,  $C_0$ ,  $C_2$ , and  $C_4$  are allowed for the longitudinal part of the form factor, and  $M_1$ ,  $M_3$ , and  $M_5$  are allowed for the transverse part of the form factor.

Figure 1 shows the individual magnetic multipoles and their incoherent sum along with the previous and present data. The solid curve drawn in Fig. 1 is a theoretical calculation with use of the wave functions of a single-particle Woods-Saxon potential of the form

$$V(r) = -V_0 f(r) - \left( \frac{\hbar}{m_\pi c} \right)^2 V_{\text{s.o.}} (\hat{\mathbf{L}} \cdot \hat{\boldsymbol{\sigma}}) \left( \frac{1}{r} \frac{d}{dr} \right) f(r), \quad (2)$$

where

$$f(r) = \{1 + \exp[(r-R)/a]\}^{-1} \quad (3)$$

with the following parameters<sup>2</sup>:  $V_0 = 52.56 \text{ MeV}$ ,  $V_{\text{s.o.}} = 5.332 \text{ MeV}$ ,  $R = 3.153 \text{ fm}$ , and  $a = 0.523 \text{ fm}$ . The well depth  $V_0$  and the spin-orbit potential depth  $V_{\text{s.o.}}$  are chosen to reproduce the  $^{17}\text{O}$  neutron binding energy (4.143 MeV) and the energy difference (5.083 MeV) between the  $d_{5/2}$  and  $d_{3/2}$  orbitals. These parameters, which are obtained from  $(d,p)$  reactions, yield an rms radius of 3.36 fm for the  $d_{5/2}$  neutron orbital. This value is smaller than the rms radius of  $3.46 \pm 0.09$  obtained

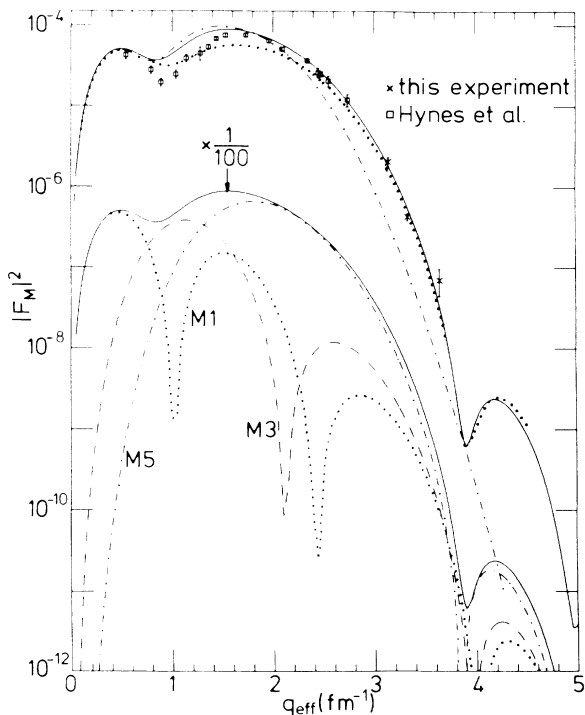


FIG. 1. The square of the magnetic form factor. The experimental data are plotted vs  $q_{\text{eff}}$ . The data of Hynes *et al.* (Ref. 6) are shown with squares, while the results of this work are represented by crosses. The lower curves show the details of the calculation with a Woods-Saxon potential:  $M_1$  multipole (dotted curve);  $M_3$  multipole (dashed curve);  $M_5$  multipole (dash-dotted curve); and the sum of all multipoles (solid curve). All these curves are reduced by a factor of 100 for clarity. The upper curves are as follows: the sum of the multipoles drawn again in actual size (solid curve); the form factor squared with use of a harmonic-oscillator potential with an oscillator constant  $b$ , of 1.8 fm (dash-dotted curve); and the form factor squared with use of the same Woods-Saxon potential with the harmonic-oscillator corrections of Ref. 7 (dotted curve).

TABLE I. The cross sections and the transverse form factors for  $^{17}\text{O}$ .

$q_{\text{eff}}$ ( $\text{fm}^{-1}$ )	Energy (MeV)	Angle (deg)	$d\sigma/d\Omega \pm \Delta(d\sigma/d\Omega)$ (mb/sr)	$ F_M ^2 \pm \Delta F_M ^2$
2.48	249.3	160.0	$1.47 \times 10^{-7} \pm 6.5\%$	$(2.50 \pm 0.18) \times 10^{-5}$
2.47	685.1	41.7	$3.24 \times 10^{-6} \pm 4.2\%$	
3.15	318.7	159.0	$7.03 \times 10^{-9} \pm 12.1\%$	$(2.11 \pm 0.26) \times 10^{-6}$
3.14	685.1	54.1	$2.55 \times 10^{-8} \pm 9.7\%$	
3.34	338.6	159.0	$1.32 \times 10^{-9} \pm 10.0\%$	$(4.41 \pm 0.46) \times 10^{-7}$
3.33	685.1	57.7	$6.15 \times 10^{-9} \pm 12.5\%$	
3.65	371.8	159.0	$1.76 \times 10^{-10} \pm 35.0\%$	$(7.07 \pm 2.63) \times 10^{-8}$
3.65	685.1	63.9	$7.85 \times 10^{-10} \pm 37.4\%$	

from the best fit to the previous data.<sup>12</sup> A calculation was also done with a harmonic-oscillator wave function with  $b = 1.8$  fm (dash-dotted curve). The center-of-mass correction and finite nucleon size are taken into account by use of the harmonic-oscillator model and the dipole fit, respectively.<sup>10</sup> As can be seen in the figure, the harmonic-oscillator calculation falls more than a factor of 5 below the data at high  $q$ . At intermediate momentum transfers, where the  $M3$  multipole is predicted to be dominant, both calculations show discrepancies with experiment. This intermediate multipole quenching seems to be universal in elastic magnetic scattering.<sup>13</sup> Taking CP and MEC into account produces an  $M3$  suppression but does not resolve the discrepancy between the data and the single-particle model form factor at intermediate momentum transfers.<sup>14</sup> A suppression of the  $M3$  multipole can also be achieved if a deformed  $^{16}\text{O}$  core is taken.<sup>15,16</sup>

The effects of processes other than the simple one-body interaction are expected to be more important at higher momentum transfers, where the extreme single-particle-model form factor falls very rapidly with increasing  $q$  (see Fig. 1). Note that for a nucleus such as  $^{17}\text{O}$ , which has an odd neutron in the stretched single-particle orbit ( $J_0 = l + \frac{1}{2}$ ), the nature of the  $M\lambda$  multipole, where  $\lambda = 2J_0$ , is determined by the radial wave function of the unpaired nucleon. The influence of configuration mixing is expected to be very small since the relevant excitations involve two-particle, two-hole states which have an energy of at least  $2\hbar\omega$  in the oscillator shell model.<sup>17</sup> This is in contrast to the  $^{13}\text{C}$  measurements where the  $M1$  multipole is not predicted by the jack-knife single-particle orbit.<sup>18</sup> First-order CP effects are also small in this region.<sup>14</sup> The data presented in this work along with those of Ref. 6 show that in the region where the  $M5$  multipole is dominant, the extreme single-particle picture is sufficient to explain the magnetic behavior. This is not the case for  $^{51}\text{V}$ , where other processes have to be taken into account in order to explain the magnetic structure of this nucleus at high-momentum transfers.<sup>19</sup>

The MEC's uniformly increase the form factor at the

peak of the  $M5$  multipole by 10%–20%.<sup>7,14,20</sup> Using calculations of MEC's, Hicks<sup>12</sup> fits the form-factor data by adjusting the strengths of the different multipoles and the radius of a Woods-Saxon potential. He finds a small effective charge of  $0.04e$  for the neutron and neglects it in his fit since the effect of CP is included in the factor that multiplies each multipole. The factor multiplying the  $M5$  amplitude is  $0.96 \pm 0.11$ , and the largest adjustment is to the  $M3$  amplitude where only  $0.53 \pm 0.06$  of the single-particle value is required. Another effect is due to three-body forces (TBF) which enhance the form factor (already corrected for CP and MEC) at the peak of the  $M5$  multipole by about 50%; however, the effect becomes smaller as the momentum transfer is increased.<sup>20</sup> It should be noted that the effect of TBF + MEC almost cancels the effect of CP in the calculation of Ref. 20.

Recent calculations by Blunden and Castel<sup>7</sup> have shown that second-order core polarization gives a suppression nearly independent of  $q$  for the  $M5$  multipole. The second-order contribution renormalizes the single-particle strength. Using harmonic-oscillator wave functions ( $b = 1.76$  fm), they show that this effect has opposite sign from the MEC and thus decreases the net effect of MEC at higher momentum transfers. These effects individually are generally less than 20% of the single-particle form factor at the peak and increase slowly with the momentum transfer.<sup>7</sup> The dotted curve in Fig. 1 shows the effect of MEC, the first- and second-order CP, and the  $\Delta$ -isobar corrections.<sup>7</sup> These effects have been added to the Woods-Saxon form factor, the square of which is represented in Fig. 1 (solid curve). This addition of harmonic-oscillator MEC and CP corrections to the Woods-Saxon prediction can only be justified qualitatively by the argument that for many-body effects, such as MEC, the momentum transfer is shared by the nucleons and thus the amplitudes should be evaluated at smaller momentum transfers where the harmonic oscillator and Woods-Saxon predictions are nearly identical. This will not be the case at very high momentum transfers. For instance, note that in the high- $q$  region,  $|F_M^{\text{HO}}|^2 \ll |F_M^{\text{WS}}|^2$ . In particular, the

secondary maximum at  $|\mathbf{q}| \approx 4.2 \text{ fm}^{-1}$  is not predicted by the harmonic-oscillator calculation.

A recent calculation,<sup>21</sup> which treats the problem relativistically, has the same general features as the curves in Fig. 1. However, it underestimates the data at high momentum transfers by more than a factor of 5. There are as yet no corrections to the single-particle picture in this relativistic calculation.

The data up to  $|\mathbf{q}| = 3.65 \text{ fm}^{-1}$  exhibit a variation of  $|F_M|^2$  by 3 orders of magnitude from the peak of the  $M5$  multipole and support a phenomenological single-particle interpretation of the  $M5$  multipole. Effects beyond the extreme single-particle picture do not seem to alter this interpretation.

The authors thank Dr. T. W. Donnelly and Dr. P. Blunden for many useful discussions. One of the authors (R.W.L.) acknowledges the support of the Fannie and John Hertz Foundation. This work has been supported in part by the U.S. Department of Energy under Contracts No. DE-AC02-76ERO3069 and No. DE-FG05-86ER40285.

<sup>(a)</sup>Present address: NIKHEF-K, P.O. Box 4395, 1009 AJ Amsterdam, The Netherlands.

<sup>(b)</sup>Present address: Department of Physics and Astronomy, University of Massachusetts at Amherst, Amherst, MA 01003.

<sup>(c)</sup>Present address: Department of Physics, Indiana University, Bloomington, IN 47406.

<sup>(d)</sup>Present address: Department of Physics, College of William and Mary, Williamsburg, VA 23185.

<sup>(e)</sup>Present address: Department of Physics, University of Washington, Seattle, WA 98195.

<sup>1</sup>F. Ajzenberg-Selove, Nucl. Phys. **A375**, 1 (1982).

<sup>2</sup>M. D. Cooper, W. F. Hornyak, and P. G. Roos, Nucl. Phys. **A218**, 249 (1974).

<sup>3</sup>S. Burzynski, M. Baumgartner, H. P. Gubler, J. Jourdan, H. O. Meyer, G. R. Plattner, H. W. Roser, I. Sick, and K. H. Möbius, Nucl. Phys. **A399**, 230 (1983).

<sup>4</sup>G. E. Brown and A. M. Green, Nucl. Phys. **75**, 401 (1966).

<sup>5</sup>I. S. Towner and F. C. Khanna, Nucl. Phys. **A399**, 334 (1983).

<sup>6</sup>M. V. Hynes, H. Miska, B. Norum, W. Bertozzi, S. Kowalski, F. N. Rad, C. P. Sargent, T. Sasanuma, W. Turchinetz, and B. L. Berman, Phys. Rev. Lett. **42**, 1444 (1979).

<sup>7</sup>P. G. Blunden and B. Castel, Nucl. Phys. **A445**, 742 (1985).

<sup>8</sup>W. Bertozzi, M. V. Hynes, C. P. Sargent, C. Creswell, P. C. Dunn, A. Hirsh, M. Leitch, B. Norum, F. N. Rad, and T. Sasanuma, Nucl. Instrum. Methods **141**, 457 (1977); W. Bertozzi, M. V. Hynes, C. P. Sargent, W. Turchinetz, and C. Williamson, Nucl. Instrum. Methods **162**, 211 (1979).

<sup>9</sup>B. E. Norum, M. V. Hynes, H. Miska, W. Bertozzi, J. Kelly, S. Kowlaski, F. N. Rad, C. P. Sargent, T. Sasanuma, W. Turchinetz, and B. L. Berman, Phys. Rev. C **25**, 1778 (1982).

<sup>10</sup>T. de Forest and J. D. Walecka, Adv. Phys. **15**, 1 (1966).

<sup>11</sup>M. Eisenberg and W. Greiner, *Excitation Mechanisms of the Nucleus* (North-Holland, Amsterdam, 1970).

<sup>12</sup>R. S. Hicks, Phys. Rev. C **25**, 695 (1982).

<sup>13</sup>T. W. Donnelly and I. Sick, Rev. Mod. Phys. **56**, 461 (1984).

<sup>14</sup>A. Arima, Y. Horikawa, H. Hyuga, and T. Suzuki, Phys. Rev. Lett. **40**, 1001 (1978).

<sup>15</sup>G. Bohannon, L. Zamick, and E. Moya de Guerra, Nucl. Phys. **A334**, 278 (1980).

<sup>16</sup>L. Zamick, Phys. Rev. Lett. **40**, 381 (1978).

<sup>17</sup>T. W. Donnelly and J. D. Walecka, Nucl. Phys. **A210**, 81 (1973); I. Sick, J. B. Bellicard, J. M. Cavedon, B. Frois, M. Huet, P. Leconte, A. Nakada, P. X. Hô, S. Platchkov, P. K. A. de Witt Huberts, and L. Lapikás, Phys. Rev. Lett. **38** 1259 (1977).

<sup>18</sup>R. S. Hicks, J. Dubach, R. A. Lindgren, B. Parker, and G. A. Peterson, Phys. Rev. C **26**, 339 (1982); R. S. Hicks, R. L. Huffman, R. A. Lindgren, G. A. Peterson, M. A. Plum, and J. Button-Shafer, Phys. Rev. C **36**, 485 (1987).

<sup>19</sup>S. K. Platchkov, J. M. Cavedon, J. C. Clemens, B. Frois, D. Gontte, M. Huet, P. Leconte, X.-H. Plan, W. Williamson, I. Sick, P. K. A. de Witt Huberts, L. Lapikás, B. Desplanques, and J. F. Maithiot, Phys. Lett. **131B**, 301 (1983).

<sup>20</sup>S. A. Coon, R. J. McCarthy, and J. P. Vary, Phys. Rev. C **25**, 756 (1982).

<sup>21</sup>E. Kim, Phys. Lett. B **174**, 233 (1986).